LAWRENCE
LIVERMORE
NATIONAL
LABORATORY

UCRL-PROC-203398

New Class of CW High-Power Diode-Pumped Alkali Lasers (DPALs)

W. F. Krupke, R. J. Beach, V. K. Kanz, S. A. Payne, J. T. Early

April 6, 2004

High-Power Laser Ablation 2004
Taos, NM, United States
April 25, 2004 through April 30, 2004

New Class of CW High-Power Diode-Pumped Alkali Lasers (DPALs)

William F. Krupke, Raymond J. Beach, V. Keith Kanz, Stephen A. Payne, and James T. Early
Lawrence Livermore National Laboratory, University of California
PO Box 808, Livermore, CA USA 94551

ABSTRACT

The new class of diode-pumped alkali vapor lasers (DPALs) offers high efficiency cw laser radiation at near-infrared wavelengths: cesium 895 nm, rubidium 795 nm, and potassium 770 nm. The working physical principles of DPALs will be presented. Initial 795 nm Rb and 895 nm Cs laser experiments performed using a titanium sapphire laser as a surrogate pump source demonstrated DPAL slope power conversion efficiencies in the 50-70% range, in excellent agreement with device models utilizing only literature spectroscopic and kinetic data. Using these benchmarked models for Rb and Cs, optimized DPALs with optical-optical efficiencies >60%, and electrical efficiencies of 25-30% are projected. DPAL device architectures for near-diffraction-limited power scaling into the high kilowatt power regime from a single aperture will be described. DPAL wavelengths of operation offer ideal matches to silicon and gallium arsenide based photovoltaic power conversion cells for efficient power beaming.

Keywords: diode, pumping, alkali, rubidium, cesium, potassium, vapor, laser

1. INTRODUCTION

High-efficiency, high-power semiconductor diode laser arrays, as pump sources for solid state lasers (SSLs), have enabled diode-pumped solid state lasers (DPSSLs) that possess greatly improved characteristics (efficiency, power, brightness, size, and weight) compared to predecessor lamp-pumped SSLs. As a result, DPSSLs have recently achieved significant and growing penetration of many commercial, medical, industrial, and military applications. Nonetheless, in pushing to ever- high powers (>kilowatt), DPSSL designers struggle to achieve near-diffraction-limited operation due to deleterious thermo-optical phenomena inherent to solid state gain media: thermally-induced focusing, stress-birefringence, and mechanical rupture. This observation prompted an inquiry as to the scientific and practical feasibility of replacing the solid state gain medium with a gaseous gain medium with relatively more favorable thermo-optical characteristics, while retaining the attractive features of high-power laser arrays as pump sources. We have identified[1] alkali vapor atoms (as a class) to offer these features when disposed in an appropriate optical configuration, based on computer models that incorporate extensive spectroscopic and kinetics cross-section data available for the alkali atoms mixed with a wide range of buffer gases. Although it is somewhat counter-intuitive, these computer models (and subsequent code validation experiments) indicate that it is feasible to design DPAL devices that will efficiently convert the relatively broadband (1-3 nm), low-brightness (M^2 ~1000) output of commercial laser diode pump arrays into high-brightness emission using alkali vapor gain media (which are characterized by relatively narrowband optical transitions of a few tenths of a nanometer, even in the presence of atmospheres of buffer gases). Moreover, due to the uniquely favorable quantum characteristics of the alkali atoms as laser gain media, this energy conversion process can be affected with a remarkably small quantum energy defect ($1-\lambda_{pump}/\lambda_{laser}$) of ~2-4%, compared to the well-known values for Nd (24%) and Yb (9%), even though a *three-level (actually, a quasi-two-level) laser scheme* is involved.

Recently, we successfully demonstrated and modeled a rubidium laser[2,3] operating on its first resonance transition at a wavelength of 795 nm, and more recently a cesium laser[4,5] operating on its first resonance transition at a wavelength of 895 nm. For both of these laser demonstrations we utilized a titanium sapphire laser as a surrogate source for a diode pump array. Using such a well-controlled pump source, we were able to quantitatively benchmark the DPAL computer codes for both Rb and Cs, based only on spectroscopic and kinetic data from the literature, and without appeal to fitting parameters. In the following sections of this paper, we first briefly review DPAL physical principles, present key DPAL design parameters, summarize key results from the rubidium and cesium laser demonstration experiments, describe DPAL device architecture options for power scaling, and describe the projected laser performance of a 2 MW DPAL, potentially useful in a earth-lunar power beaming application.

2. DPAL PHYSICAL PRINCIPLES

As a class, the neutral alkali vapor atoms (Li, Na, K, Rb, and Cs) manifest the same rather simple low-lying electronic structure, due to their possession of but a single valance s-electron. This electron gives rise to a $^2S_{1/2}$ ground level and to $^2P_{1/2}$ and $^2P_{3/2}$ first and second excited levels split by a relatively small energy due to spin-orbit interaction. For illustrative purposes here we use the rubidium atom whose energy levels are shown in Fig. 1. The spectroscopic properties of the electric-dipole allowed $^2S_{1/2}$-$^2P_{1/2}$ and $^2S_{1/2}$-$^2P_{3/2}$ resonance transitions (the so-called D_1 and D_2 transitions, respectively) of the alkali atoms have been extensively studied[6]. The collisional effects of all of the rare-gases and selected molecular gases on the population kinetics of $^2P_{1/2,3/2}$ excited alkali atoms, including spectral broadening of the D-transitions, collisional mixing rates of excited $^2P_{1/2,3/2}$ alkali atoms, and inelastic quenching rates have also been reported in the litereature[7].

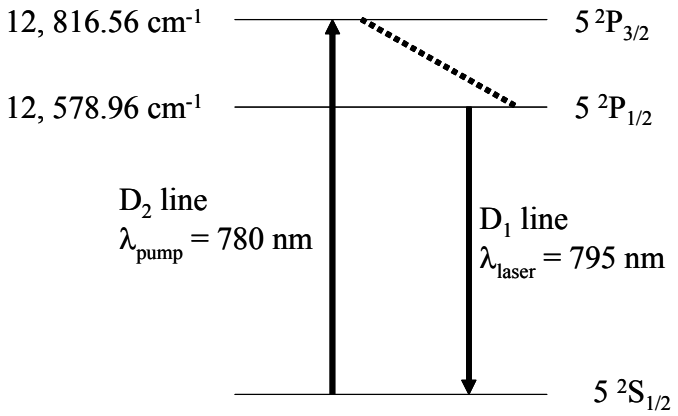

Fig. 1 Energy level diagram of atomic Rb indicating pump and laser transitions.

In a DPAL, the D_2 transition is the pump transition, and the D_1 transition is the laser transition. Note that both levels of the laser transition have the same degeneracy (2) and that the terminal level of the laser transition is the unsplit ground level. Note also that the terminal level of the pump transition has twice the degeneracy (4) as that of the initial pump transition level. Table 1 lists for the potassium, rubidium, and cesium alkali vapors the D_2 pump wavelengths, the D_1 laser wavelengths, ^2P energy splittings, and quantum energy defects, $(1- \lambda_{laser}/\lambda_{pump})$. These alkalis are of particular interest because they can all be pumped with mature laser diode arrays utilizing AlGaAs and InGaInP compound semiconductor material systems.

Table 1. DPAL pump and laser wavelengths, energy gaps, and quantum defects.

Alkali Atom	λ_{pump} (nm)	λ_{laser} (nm)	$^2P_{3/2}$-$^2P_{1/2}$ Energy Gap (cm^{-1})	Quantum Defect
K, potassium	766	770	57.7	0.0044
Rb, rubidium	780	795	237.5	0.019
Cs, cesium	852	895	554.1	0.047

Because of the relatively small energy difference between the D_1 and D_2 transitions of each alkali atom (~2% for Rb, ~5% for Cs), these atoms have the potential to be especially efficient laser species. Note also that, because the energy gaps between the $^2P_{3/2}$ and $^2P_{1/2}$ levels are comparable to kT at room temperature (~210 cm^{-1}), the $^2P_{3/2}$ and $^2P_{1/2}$ levels will tend to be in Boltzman equilibrium, and that therefore a DPAL operates essentially in a *quasi-two-level* laser scheme. Population inversions on the D_1 transition have been reported using narrowband laboratory pump sources[8-11]. The challenge before us is to assess and devise a practical mean for effectively pumping a DPAL with relatively broadband laser diode arrays. For efficient quasi-two-level laser action to be achieved in alkali atoms pumped by commercial multimode diode pump laser sources with spectral widths a large as several nm, three conditions need be met simultaneously. First, diode pump energy must be efficiently absorbed in the relatively narrow D_2 transition; second, the excitation energy must be rapidly and efficiently transferred to the upper laser level (without sustaining significant fluorescence or quenching of excitation energy back to the ground level); third, excitation energy has to be efficiently extracted in the D_1 resonance transition without burning a spectral hole. To avoid the latter, the D_1 and D_2 transitions must be collisionally broadened sufficiently (see criterion below) to assure that these transitions are

effectively spectrally homogeneous to pump and induced D_1 laser radiation fluxes. This can be achieved by buffering the alkali vapor with a rare gas such as helium at moderate pressure. Even when so collisionally broadened, D_2 transition widths are still many times narrower than the spectral widths of practical pump diode arrays. This linewidth disparity can be overcome, and a high absorbed-fraction of pump radiation can be achieved, by adopting an "end-pumped" laser geometry. In this geometry, the opacity of the medium in the far spectral wings of the D_2 transition can be made sufficiently large (by setting the product of alkali density and vapor column length appropriately), resulting in very high pump absorption efficiencies. Once pump energy is efficiently absorbed, population excited to the $^2P_{3/2}$ level must be rapidly transferred to the $^2P_{1/2}$ upper laser level at a rate that is much faster than ^2P spontaneous emission rates of ~ 3 x 10^7 sec^{-1}. Collisional mixing of the $^2P_{1/2,3/2}$ levels at rates an order of magnitude greater than this can be achieved by buffering the alkali vapor with ~100 Torr partial pressure of a small molecule such as ethane[12]. Having outlined an approach to achieving these three conditions simultaneously, one can anticipate *efficient diode-pumped* laser action on the first resonant D_1 transitions of the alkali atoms.

3. DPAL DESIGN PARAMETERS

We have seen that one of the critical requirements necessary to the realization of an efficient DPAL device is that the D_2 pump transition be effectively spectrally homogeneous. Under physical conditions of interest to DPAL operation, the degree of spectral homogeneity of the D_2 pump transition is determined by the gas temperature and by the partial pressure of a buffer gas such as helium. In the limit of no helium buffer gas, the spectral character of the D_2 pump transition is determined essentially by Doppler broadening. The transition line-shape is Gaussian and the transition is spectrally inhomogeneous. In the presence of a sufficiently large partial pressure of helium buffer gas, collisions of the alkali atoms with the buffer gas atoms broaden and reshape the D_2 pump transition. When buffer gas collisions so dominate, the D_2 pump transition line-shape becomes Lorentzian and the transition becomes effectively spectrally homogeneous. For our purposes here we can take the D_2 pump transition as effectively spectrally homogeneous when the collision-broadened linewidth is at least 10 times the Doppler linewidth. Once the pump transition becomes spectrally homogeneously broadened, pump radiation absorbed in the spectral wings of the pump transition contribute to DPAL laser gain just as effectively as pump radiation absorbed within the spectral half-width of the transition. This is important because it is impractical to collisionally broaden D_2 pump transitions so much that they are as broad as, or broader than, the typical spectral widths of commercial high power laser diodes. Thus, in designing practical DPAL devices there are always design tradeoffs to be made involving the helium buffer pressure and the spectral width of the pump laser diode array. In general, one is required to provide a certain minimum helium partial pressure to ensure that the D_2 pump transition is spectrally homogeneous. Higher helium partial pressure can then be utilized to accommodate even larger spectral widths of pump laser diode arrays.

The minimum helium buffer pressures for K, Rb, and Cs have been calculated, for which the D_1 and D_2 collisionally broadened Lorentzian linewidths are 10 times the Doppler broadened linewidths, and presented in reference 13 and reproduced here in Table 2.

Table 2. K, Rb, and Cs critical helium partial pressures to render the D_2 pump transitions effectively spectrally homogeneous.

Alkali Atom	$P_{homogeneous}$ (atm)	$\Delta\lambda_{L,\,min}$ (nm)
K, potassium	0.436	0.0164
Rb, rubidium	0.420	0.0116
Cs, cesium	0.264	0.0102

From Table 2 we see that the D_2 pump transition becomes effectively spectrally homogeneously broadened at helium partial pressures of a few tenths of an atm, and that the corresponding linewidths (FWHM) are approximately 0.01 nm. Pump source whose spectral width is larger than 0.01 nm may thus be utilized to effectively pump a DPAL, by virtue of predominantly wing-pumping of the D_2 pump transition.

4. DPAL DEMOSTRATION EXPERIMENTS USING A TiS SURROGATE PUMP SOURCE

Recently we reported CW TEM_{00} laser action at 795 nm on the D_1 transition of rubidium[2,3], using a titanium sapphire pump laser as a surrogate for a diode pump. The spectral width of the TiS pump was about four times broader than the collisionally broadened D_2 pump transition. We modeled the end-pumped geometry utilized in this laser demonstration experiment using the methodology developed by Beach[14] for CW end-pumped quasi-three-level lasers such as Yb:YAG. We assume plane waves for the pump and laser beams within the resonator, and spectrally convolve the broader spectrum of the pump with the narrower Lorentzian pump transition of the alkali vapor along the cell, taking into account depletion of the ground level and the spectral reshaping of the pump beam as it propagates through the absorbing atomic vapor. We obtained excellent quantitative lock-up with the code using literature spectroscopic and kinetic data[5].

More recently, we reported CW TEM_{00} laser action at 895 nm on the D_1 transition of cesium[4,5], using a titanium sapphire pump laser as a surrogate for a diode pump. Fig. 2 graphs the observed output power at 895 nm versus pump power, using output couplers with differing reflectivities.

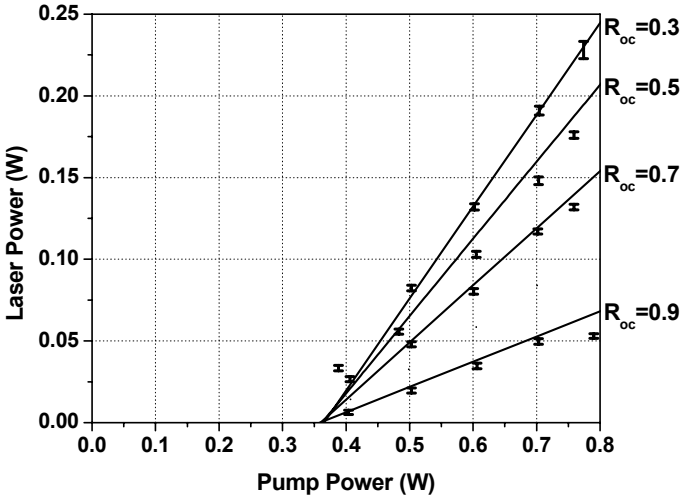

Fig. 2. Laser output at 895 nm of a Titanium sapphire laser pumped cesium laser.

To assess the performance of this cesium laser we have measured output laser power against incident pump power for a series of output couplers having reflectivity values of 0.3, 0.5, 0.7 and 0.9 at 895 nm. The Ti:Sapphire pump could deliver up to 800 mW of pump light, and for each output coupler we measured laser output power for varying pump input power. Plotted in Fig. 2 as the data points, is our measured laser output power vs. pump input power for the series of output couplers we evaluated. The pump power on this plot is measured before the cell and is delivered into the cell with an efficiency of 0.9 from that point. The best performance was achieved with the 0.3 reflectivity output coupler, giving a peak optical-optical conversion efficiency of 0.34 W/W and a slope efficiency of 0.59 W/W relative to the absorbed pump power. Using spectroscopic and kinetic data appropriate to cesium, our rate equation model gives the straight line predications in Fig. 2 for the Cs laser output power vs. pump input power. The good agreement between experiment and model evident in Fig. 2 is achieved without the use of any adjustable parameters. This gives us confidence that we have included all the necessary physics relevant to this laser, and that we can confidently use the developed model to extrapolate system performance.

An experiment to demonstrate a potassium DPAL resonance laser at 770 nm using a TiS surrogate pump, designed using literature spectroscopic and kinetic data, is anticipated in the near future. Model calculations indicate that a potassium DPAL may ably fulfill the role of laser source for a potassium guidestar, according to the analysis of Papan[15].

5. DPAL DEVICE ARCHITECTURES FOR POWER SCALING

Using these Rb and Cs benched-marked models we have modeled end-pumped DPAL systems in which the pump freely propagates through a vapor "cell" as shown in Fig. 3. In this approach, a hollow lens-duct is used to deliver the pump light to the laser cell in a way that is compatible with both the use of a geometrically unstable resonators, and the desire to let the pump light double pass the gain medium to improve pump absorption efficiency. The gain cell may take the form of a circularly-symmetric capillary or tube with radius r_0, or the gain cell may take the form of a thin planar

waveguide of thickness, 2δ, and width, w, (extending perpendicular to the page). Here, two basic power-scaling schemes are considered: 1) the alkali/He-buffer gain medium is static within the gain cell, and waste heat is transported to the cell walls by thermal conduction in the helium buffer gas; and 2) the alkali/He-buffer gain medium is flowed axially through a cylindrical gain cell, and waste heat is convectively removed as the heated gain medium exits the cell.

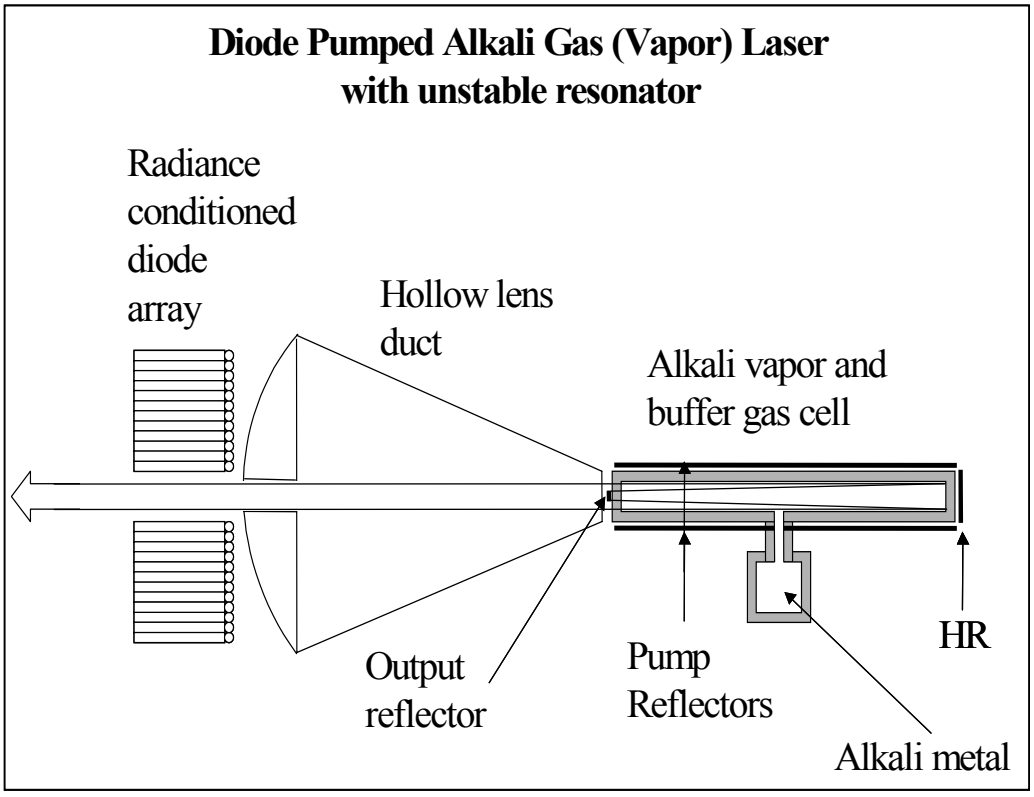

Fig. 3. Architecture for DPAL power scaling

5.1.Static-gas, conductive-cooling, planar waveguide DPAL configuration.

The static gain medium scheme is relatively simple and compact, but will be restricted in achievable output power with high beam quality (compared to the convective cooling scheme, see section 5.2 below) due to the fact that the induced transverse temperature gradient must to be restricted to some maximum tolerable value. To maximize the high-brightness output power in the static scheme, the planar waveguide gain cell configuration (Figure 4) is adopted, ensuring that one of the gain cell's dimensions is small, thus facilitating the transfer of waste heat to the two near-by, relatively large, cooling surfaces with a minimal temperature gradient. In this design, diode pump radiation is delivered through a hollow lens duct and the slab configured gain volume is extracted using a zigzag geometry. Prismatic windows on the gain cell are used to enable a zigzag path without deviating the light path outside of the gain cell.

Preliminary analyses of the high-brightness power scaling of Rb and Cs lasers employing a static gain medium in the planar waveguide configuration have been reported[5, 13]. The parametric dependences of output power with helium buffer pressure and pump diode array linewidth were also explored. These analyses indicate that high beam quality power scaling of Rb and Cs lasers well into the multi-kilowatt regime seems practical, perhaps to powers as high as 100 kW, with projected opt-to-opt conversion efficiencies perhaps as high as 50-70%. In addition to this laser oscillator design, model calculations also indicate that a diode-pumped alkali gain medium can be efficiently utilized in a classic master-oscillator, power-amplifier (MOPA) configuration because high saturated gain gains (>200x) appear achievable.

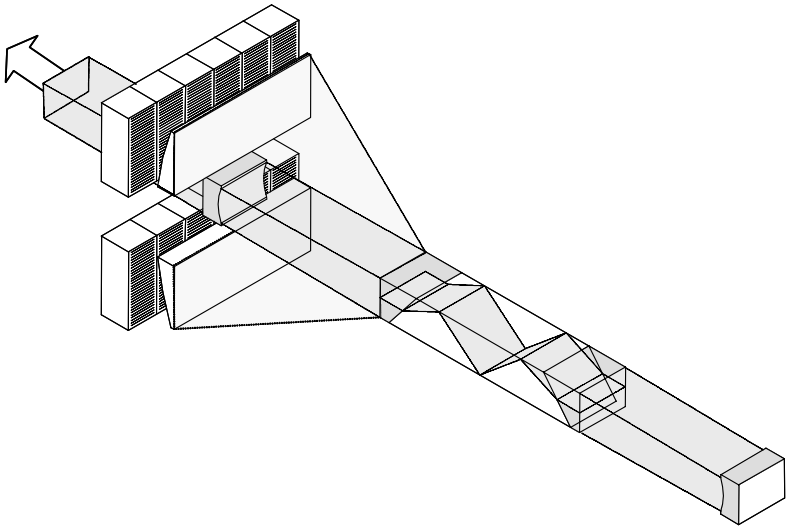

Fig. 4. DPAL planar waveguide cell configuration in which the gain medium is static.

5.2. Flowing-gas, convective-cooling, cylindrical tube DPAL configuration.

To scale high-brightness DPAL power to the megawatt range (for use in power beaming applications, for example) it will be necessary to flow the gain medium through the gain cell and convectively remove waste heat (Figure 5). For convective cooling, the small heat loads relative to the gas thermal capacity will allow low flow rates and low temperature increases.

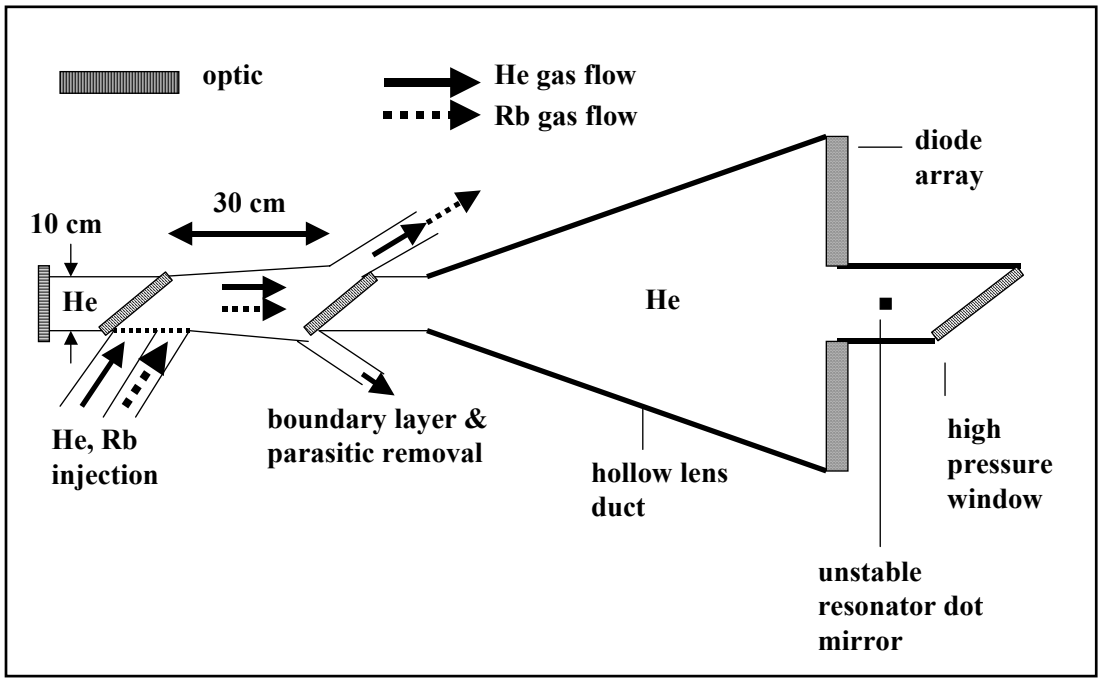

Fig. 5. DPAL cylindrical cell configuration in which the gain medium is flowed axially.

The walls of the lens duct that transports radiation from the diode pump array to the laser cavity, and the walls of the laser cavity, need to be highly reflective at the pump wavelength, so as to efficiently couple the diode pump power into the laser gas. There will be some loss of photons through the gas inlet and exit orifices, but the output plane of the diode pump array will be the primary surface that absorbs pump photons not deposited in the laser gain medium. Since the diode pump array structure itself will be water-cooled, the additional heat load is not anticipated to be a major thermal design driver of the diode array.

Because of its quasi-two-level nature, with a large resonant loss when not strongly pumped, alkali vapor must be confined only to the pumped portion of the laser cavity. Figure 5 shows a configuration in which both the pump light transport lens duct volume, and the opposing resonator optics cavity, are filled with helium. A window separates these cavities from the cavity containing the laser medium. These windows can be very thin if the pressures on either side are equal. The use of thin optics would minimize absorption by the optics, and thus minimize the heating of the optics and any resulting optical distortions. It would also avoid any optical distortions from structural loads. If by contrast these adjacent cavities are at low pressures or vacuum, these windows might have to bear the up to several tens of atmospheres of laser medium pressure. The configuration of Fig. 5 shows this mechanically-stressed optic as the output window.

Figure 6 shows a schematic layout of the associated gas flow loop (and some projected typical temperature and pressure values; see below section 7). The viscous losses along the walls are expected to be modest, and the mechanical pump requirements should be small. A simple heat exchanger section will also be required to remove the excess heat. The number density of the alkali vapor will be controlled in most of the flow loop by simply keeping the wall temperature about the temperature required for the equilibrium alkali vapor density. This will prevent the vapor from depositing on any surface in the flow loop. There will also be a section where the vapor is brought in contact with a reservoir of liquid alkali. A feedback loop will adjust the alkali reservoir temperature to control the alkali vapor density in the laser gas.

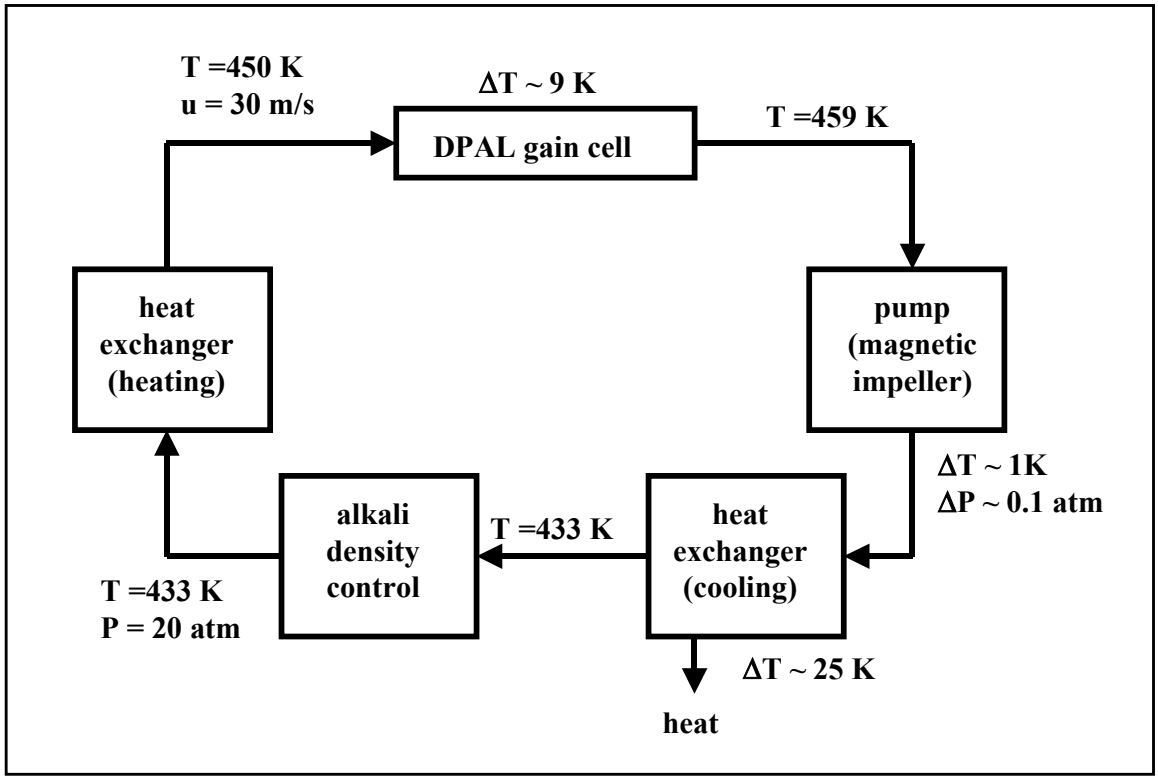

Fig. 6. Schematic layout of a high power DPAL flow cooling loop.

6. OPTIMAL LASER WAVELNGTHS FOR POWER BEAMING

One of the attractive applications for a high power (megawatt-class) DPAL is power beaming over extended distances (for example providing sustaining operating power from the earth to a lunar base[16]). Fig. 7 shows the spectral dependence of PV conversion efficiency of Si, GaAs and other semiconductor materials[17]. The long-wavelength threshold for excitation of a silicon PV cell is ~1100 nm, rises to a peak conversion efficiency of ~40% at a wavelength of ~900 nm, and drops to half-peak conversion efficiency at a wavelength of ~500 nm. It is known that silicon PV cells exposed to electron bombardment characteristic of the GEO environment are damaged in a manner that decreases the PV efficiency and shifts the spectral response curve to shorter wavelengths. Thus, the optimum operating wavelength of a laser power beaming source employing silicon PV cells is ~900 nm (if the silicon PV cells will not be subjected to damaging electron irradiation); the optimum wavelength shifts to ~770 nm when such damage is anticipated. The GaAs PV cell exhibits a long-wavelength excitation threshold of ~910 nm, rises to a peak conversion efficiency of ~60% at a wavelength of ~850 nm, and drops to half-peak conversion efficiency at a wavelength of ~300 nm. Thus, for GaAs PV cells, the optimum source wavelength is ~850 nm, but a source operating wavelength of ~800 nm will not result in a significantly lower efficiency. DPALs are therefore particularly attractive for such applications because the alkali laser wavelengths (Table 1) are well matched to excitation peaks of Si and GaAs photovoltaic cells.

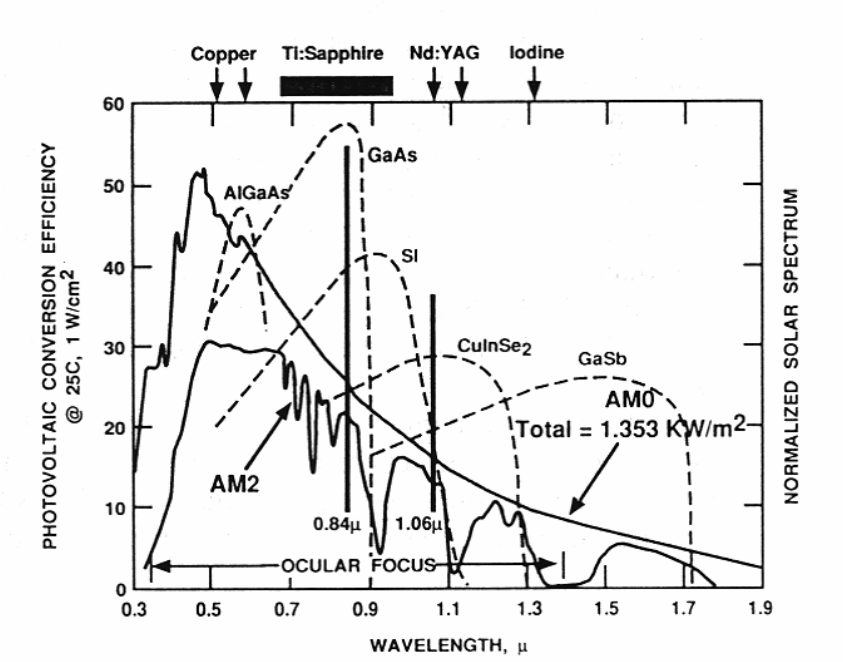

Fig. 7. Spectral response of photovoltaic cells (after ref. 17).

Solar cells are designed to operate under steady continuous-wave (CW) solar illumination. Illumination for the cell produces useful electric power proportional to the photocurrent, while producing a dissipative power loss proportional to the square of the photocurrent (due to the cell's internal resistance). For a specified illumination intensity, the cell is designed to maximize conversion efficiency. When illuminated by a repetitively pulsed source with a given peak to average intensity, the dissipative power loss increases relative to useful power generated, thus lowering the cell conversion efficiency. The degree to which efficiency decreases depends strongly on the peak-to-average power of the rep-pulsed source, the characteristic time duration of the pulses, and the internal response time of the cell photoelectrons[18, 19, 20]. Simulations of Si and GaAs photovoltaic cell responses to pulsed waveforms have been carried out[21] and correlated with measurements of cell performance under pulsed illumination. In summary, these studies show that: 1) cell performance degrades significantly for sources generating long pulses (>25 nsec) at low duty factors (<0.001); 2) cell performance may degrade incrementally for sources generating short pulses (<100 psec) at high duty

factor (>0.1); and 3) the optimum power beaming source temporal waveform is continuous wave (CW). Since DPALs operate in a purely CW mode, their output waveform is also optimally matched to driving Si and GaAs photovoltaic cells.

7. NOMINAL DESIGN PARAMETERS FOR A 2 MW Rb DPAL

The nominal laser design parameter values have been assessed for a megawatt-class DPAL with the flow-cooled cylindrical gain cell architecture. Table 3 lists key parameter values for a 2 MW DPAL point design laser the design.

Table 3. 2MW DPAL point design parameters and performance

Parameter	Value	Units
gain cell length	30	cm
gain cell diameter	11	cm
laser mode diameter	10.8	cm
laser mode volume	2750	cm^3
laser mode output area	91.6	cm^2
helium pressure (T = 20 C)	20	atm
ethane pressure	100	torr
rubidium density	4.3×10^{13}	cm^{-3}
rubidium cold temp	160	C
pump power	3.7	MW
pump wavelength	780	nm
pump line-width	2.0	nm
pump delivery efficiency	0.95	
pump irradiance	37	kW cm^{-2}
pump reflectivity coefficient	0.99	
pump absorption efficiency	82.5	%
one-way transmission	0.99	
pump mode fill fraction	0.964	
output power	2.07	MW
out-coupler reflectivity	0.20	
output power irradiance	22.5	kW cm^{-2}
optical conversion efficiency	55.8	%
fluorescence power	0.765	MW
waste heat density	17	watt cm^{-3}
gain medium flow velocity	30	m/sec
Mach number	0.024	
gain medium temperature rise	9	C

The rise in temperature, ΔT, of the alkali-buffer gain medium as it transits the pumped volume is given by:

$$\Delta T = f_{heat} I_{pump} L A \{m C_p u\}^{-1} \quad (1)$$

where

m = mass of helium in the pumped cavity
f_{heat} = fraction of absorbed pump power converted to heat
I_{pump} = pump intensity
u = flow speed of the gain medium through the pumped cavity
C_p = specific heat of helium
L = length of the pumped cavity
A = area of the pumped cavity

For the present point design, we have assumed the modest flow velocity of u = 30 m/sec. The pumped cavity is assumed to have a length of 30 cm, and diameter of 11 cm (pump cavity area of 92 cm^2). For the assumed pump intensity of 37 $kW\text{-}cm^{-2}$, the fraction of absorbed pump power converted into waste heat is calculated to be f_{heat} =0.013. The mass of helium in the pumped cavity is 10.2 grams, and using the specific heat value for helium of 5.2 joules/gm-K, Eq. (1) yields a temperature rise during transit through the pumped cavity of $\Delta T = 9^oK$.

The Reynolds number is approximately one million, so the flow will be turbulent. For the cavity temperature of 450^oK, the sonic velocity in helium is 1245 m/s giving a very low Mach number, M, of 0.024. At such a low Mach number compressibility will not be an issue. The dynamic temperature variation is only

$$(T_o - T) = 0.5\,(\gamma\text{-}1)\,M^2\,T_o = 0.08^oK \qquad (2)$$

Thus, density variations due to turbulence or dynamic temperature recovery in the boundary layer do not appear to be important. The main temperature variations will be due to the lower velocities and the resulting high pump power absorption in the velocity boundary layer. The boundary layer thickness is estimated to be about 7 mm at the exit end of the gain cell. The gain cell is envisioned to incorporate a slight diameter expansion to provide a dump for near-axially directed ASE. Thus, the heated boundary layer is expected to be largely outside of the laser extraction volume, but this issue requires detailed analysis and evaluation.

The primary concern regarding the gas flow is a possible separation of the flow from the cell walls, and the establishment of flow recirculation regions. Gas in the recirculation region would continue to heat and would strongly affect laser performance. The flow will have to be carefully injected into the flow cavity to avoid separation as it turns to flow parallel to the cell axis. The use of flow guide-vanes or distributed flow injection along the walls may be required. As mentioned above, because of the high saturated power gains that appear possible from the alkali-buffer gain medium, it may turn out that megawatt class laser devices might adopt a MOPA optical configuration.

6. CONCLUSIONS

The possibility of realizing efficient, compact diode-pumped alkali lasers (DPALs) has been investigated conceptually and computationally, and validated for rubidium and cesium using a titanium sapphire surrogate source for a diode pump array. Validated DPAL device design codes for rubidium and cesium have been utilized to numerically explore the design parameters of multi-kilowatt class DPAL devices, and to project their optical and thermal characteristics. These preliminary design studies indicate that multi-kilowatt (and even megawatt-class) DPALs with optical-optical efficiencies greater than 50% are feasible with good beam quality, using commercial diode pump arrays, and practical opto-mechanical configurations.

6. ACKNOWLEDGEMENTS

This work was performed under the auspices of the U. S. Department of Energy and the University of California by Lawrence Livermore National Laboratory under Contract No. W-7405-ENG-48. We would like to thank our Army Research Laboratory colleagues, Mark Dubinskii and Larry Merkle, for their help and participation in the Cs-laser studies reported in Refs. 4 and 5, as well as the Joint Technology Office for their support of this work.

7. REFERENCES

1. W. F. Krupke, Diode-Pumped Alkali Laser, US Patent No. 6,643,311 B2
2. W.F. Krupke, R.J. Beach, V.K. Kanz, and S.A.Payne, "Diode Pumpable Rubidium Laser," OSA TOPS Vol. 83, Advanced Solid-state Photonics pp. 121 (2003)
3. W. F. Krupke, R. J. Beach, V. K. Kanz, and S. A. Payne, "Resonance transition 795 nm rubidium laser", Optics Letters, **28**, 2336-2338 (2003).
4. R. J. Beach, W. F. Krupke, V. K. Kanz, M. A. Dubinskii, and L. D. Merkle, "End-pumped 895 nm Cs laser", Advanced Solid State Photonics (ASSP) meeting, Feb 2-4, 2004.
5. R. J. Beach, W. F. Krupke, V. K. Kanz, M. A. Dubinskii, and L. D. Merkle, "End-Pumped Alkali Vapor Lasers: Experiment, Model, and Power Scaling", submitted Feb 2004 for publication, JOSA B.
6. P. S. Doidge, "A Compendium and Critical Review of Neutral Atom Resonance Line Oscillator Strengths for Atomic Absorption Analysis", Spectrochmica Acta., **50B**, 209 (1995).
7. L. Krause, "Collisional Excitation Transfer Between the $^2P_{1/2}$ and $^2P_{3/2}$ Levels in Alkali Atoms", Applied Optics, **5**, 1375 (1966).
8. B. A. Glushko, M. E. Movsesyan, and T. O. Ovakimyan, "Processess of Stimulated Electronic Raman Scattering and Stimulated Resonance Emission in Potassium Vapor in the Presence of a Buffer Gas". Opt. Spectrosc (USSR), **52**, 458 (1982).
9. Konefal and M. Ignaciuk, "Stimulated Processes in Sodium Vapor in the Presence of Molecular Buffer Gas Systems", Opt. And Quantum Electronics, **28**, 169 (1996).
10. M. E. Movsesyan, T. O. Ovakimyan, and S. V. Shmavonyan, "Stimulated Processes in a Mixture of Rubidium Vapor and Buffer Gas Under Two Photon Excitation", Opt. Scpetrosc (USSR), **61**, 285 (1986).
11. A. M. Davtyan, M. E. Movsesyan, A. V. Papoyan, and S. V. Shmavonyan, "Laser Resonance Radiation at the Atomic-Potassium D1 Line", Opt. Spectrosc (USSR), **66**, 686 (1989).
12. E.S. Hrycyshyn and L. Krause, "Inelastic collisions between excited alkali atoms and molecules. VII. Sensitized fluorescence and quenching in mixtures of rubidium with H_2, HD, D_2, N_2, CH_4, CD_4, C_2H_4, and C_2H_6," Can. J. Phys. **48**, pp. **2761** (1970).
13. W. F. Krupke, R. J. Beach, V. K. Kanz, and S. A. Payne, "DPAL: A new class of CW, near-infrared, high-power diode-pumped alkali (vapor) lasers", Photonics West Symposium, Jan 2004, SPIE **5334**, to be published.
14. R.J. Beach, 'CW Theory of Quasi-Three Level End-Pumped Laser Oscillators,' Optics Communications **23**, 385-393 (1995)
15. G. Papen, C. Gardner, and W. M. Pfenninger, Appl. Optics, **34**, 6950 (1995).
16. G. A. Landis, "Solar Power for the Lunar Night", NASA TM-102127, May, 1989.
17. H. E. Bennett, "Free-electron laser power beaming to satellites at China Lake, California", Nuclear Inst. and Methods in Phys. Res., **A341**, 124-131 (1994)
18. G. W. Zeiders, "Systems Analysis on Laser Beamed Power". NASA-CR-193206, NASA Contract H-11986D, April 1993
19. B. Anspaugh, R. Mueller, R. Lowe, and G. A. Landis, "Results of Illuminating Various Solar Cells with Pulsed Laser Light", JPL Publ. 92-25, Nov. 1, 1992
20. R. Lowe, G. A. Landis, and P. Jenkins, "The Efficiency of Photovoltaic Cells Exposed to Pulsed Laser Light", Proc. XII Space Photovoltaic Research and Technology Conf. (SPRAT XII), NASA CP 3210, 129-146, Oct., 1993
21. R. K. Jain and G. A. Landis, "Modeling of High Efficiency Concentrator Solar Cells Under Laser Pulse", Laser Power Beaming, SPIE, **2121**, 264-268 (1994)